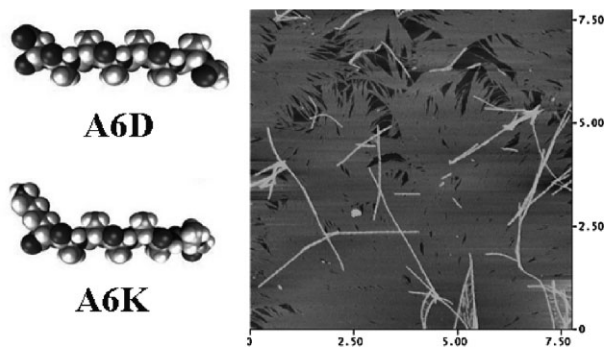


Synergistic Effect and Hierarchical Nanostructure Formation in Mixing Two Designer Lipid-Like Peptide Surfactants Ac-A₆D-OH and Ac-A₆K-NH₂

Ulung Khoe,^a Yanlian Yang,^a Shuguang Zhang*

We here report the nanostructures from combinational self-assembly of two designer lipid-like peptides Ac-A₆D-OH and Ac-A₆K-NH₂ using dynamic light scattering (DLS) and atomic force microscopy (AFM). The synergistic phenomenon is observed by measuring the critical aggregation concentrations (CACs) of these two mixed peptides, in different molar ratios by DLS. The nanoropes were observed in AFM images at a molar ratio of Ac-A₆D-OH/Ac-A₆K-NH₂ = 1:1, and the thin film formation with aligned nanoropes is shown at a molar ratio of 2:1. The well aligned nanoropes at the molar ratio of Ac-A₆D-OH/Ac-A₆K-NH₂ = 2:1 indicated the competition factor between the electrostatic repulsion according to DLVO theory and the hydrophobic interaction arising from the long side chains on lysine residues. This study will further our understanding for designing new nanomaterials based on designer lipid-like peptide surfactants.



Introduction

Nanofibers and nanotubes self-assembled from designer peptides and proteins have attracted considerable atten-

tion of researchers in different fields. Nanostructured biomaterials from self-assembly of DNA, peptides, and proteins have demonstrated potential applications in biosensors, controlled release medicine, 3-D cell cultures, reparative and regenerative medicine, as scaffold to organize metal nanocrystals and fabricate metal nanowires and more.^[1,2]

Some nanofibers from different protein assemblies are found in a number of amyloid diseases.^[3,4] Much work has been carried out not only to understand how these nanofibers aggregate, but also to find means to inhibit the amyloid formation. On the other hand, some peptide and protein nanofibers have applications as scaffolds for material science and nanotechnology.^[1,2] Thus, a detailed understanding and knowledge of the mechanism of the well-formed nanostructures including nanofiber and

U. Khoe, Y. L. Yang, S. G. Zhang

Center for Biomedical Engineering NE47-379, Massachusetts Institute of Technology, 77 Massachusetts Avenue, Cambridge, Massachusetts 02139, USA

Y. L. Yang

National Center for Nanoscience and Technology, Beijing, 100190, China

S. G. Zhang

Center for Bits & Atoms, Massachusetts Institute of Technology, 77 Massachusetts Avenue, Cambridge, Massachusetts 02139, USA

Fax: (+1) 617 258 5239; E-mail: shuguang@mit.edu

*These two authors contributed equally.

nanorope, nanotube formation will be valuable for the design and controlled-fabrication of nanostructured materials.

We previously reported^[5–9] self-assemblies of several lipid-like peptide surfactants including Ac-G₄D₂-OH, Ac-G₆D₂-OH, Ac-G₈D₂-OH, Ac-A₆D-OH, Ac-V₆D-OH, Ac-I₆D₂-OH, Ac-A₆K-NH₂, Ac-V₆K-NH₂, Ac-V₆R-NH₂, Ac-I₆RR-NH₂, and Ac-L₆RR-NH₂. This class of lipid-like self-assembling peptide surfactants has a hydrophobic tail with several consecutive hydrophobic amino acids at N-terminus, for example, glycine, alanine, valine, and leucine; and a hydrophilic head with one or two hydrophilic amino acids at C-terminus, with either a negatively charged aspartic acid or a positively charged lysine. When dissolved in water or aqueous solutions, these peptides undergo self-assembly to form particles, nanovesicles, or nanotubes.^[5–9] They are not only useful for stabilizing membrane proteins outside the cell membrane,^[10–13] but also be useful for water-insoluble drug formulations because of their surfactant properties. Furthermore, since it has lipid-like properties, it has been shown that this class of peptides interacts well with lipids.^[14] These peptide nanotubes are of special interest for their potential uses as drug and gene delivery vehicles, scaffold for coating metal nanowires, and artificial transmembrane channel, and for the stabilization of membrane proteins.^[10–13]

Similar to common surfactants, these lipid-like peptide surfactants have defined critical aggregation concentrations (CACs) in submillimolar to millimolar range, depending on the hydrophobicity of the tails, the geometry, shape, and charges of the heads and the ionic concentration as well.^[12–14] The unique property of this class of lipid-like peptide is that they can be exquisitely fine-tuned both for their tails and heads. For example, they can retain the same tail length of six amino acids, ≈ 2 nm, but can vary the hydrophobicity broadly, thus a wide range of CACs.

In the literature, synergistic effects have been reported by combining common surfactants, especially combining cationic and anionic surfactants at various ratios to lower CAC value than those of the individual surfactants.^[15,16] This phenomenon is mainly due to the entropic free energy contributions related with the surfactant head groups. The synergistic effects in mixtures of an anionic and a cationic surfactant have been observed to give rise to enormous synergism, which may be ascribed to the elimination of the unfavorable electrostatic free energy.^[15,16] Because the lipid-like peptides resemble many surfactants, both chemically and structurally, they have similar self-aggregation behavior, including CAC ranges, particle, vesicle, nanorod, and nanotube formations. We reasoned perhaps by mixing the cationic and anionic peptide surfactants with the same hydrophobic tails, there might be an observable increase for the surface activity of these

peptide surfactants. The synergistic effects may also be helpful for the controlled assembly of the peptide nanovesicles, nanotubes, and nanoropes. Thus, it could provide another avenue for the design of nanostructured materials.

Several lipid-like peptide surfactants have been reported to self-organize themselves into highly ordered nanotube structures in aqueous solutions at a certain pH, and the nanotube structures have been studied by transmission electron microscopy (TEM) using quick-freeze/deep-etch sample preparation method and atomic force microscopy (AFM) method as well.^[5–9] We here report the synergistic effect of mixing the peptide surfactants, Ac-A₆D-OH and Ac-A₆K-NH₂, in different molar ratios studied by AFM and by dynamic light scattering (DLS) methods. We observed rather uniformed nanoropes under AFM imaging at the molar ratio of Ac-A₆D-OH/Ac-A₆K-NH₂ = 1:1. Furthermore, the thin film formation with aligned nanoropes was found to be in the molar ratio of 2:1.

Experimental Part

Peptide Design and Synthesis

The lipid-like peptides have a hydrophilic head and a hydrophobic tail. The length of the hydrophobic tail is modeled to be approximately of the size of phospholipid, ≈ 2.4 nm. The hydrophilic head can be chosen from anionic or cationic amino acids. Two kinds of lipid-like peptides, Ac-AAAAAAD-OH (Ac-A₆D-OH) and Ac-AAAAAAK-CONH₂ (Ac-A₆K-NH₂), are used in the experiments. Their molecular models are shown in the inset in Figure 1A. These two peptides were chosen with good solubility in water. For both the two peptides, hydrophobic tails consist of six alanine residues, so the tails are identical both biochemically and structurally. The only difference is their hydrophilic heads. Ac-A₆D-OH has an acidic head aspartic acid with two negative charges at pH 7, while Ac-A₆K-NH₂ has a basic head lysine with positive charge at pH 7.

These peptides were commercially synthesized by CPC Scientific Inc., CA. These peptides were solubilized in Milli-Q water to a concentration of 16×10^{-3} M (Ac-A₆K-NH₂) and 4.8×10^{-3} M (Ac-A₆D-OH) and the pH values were adjusted to 7 and 12, respectively with NaOH or HCl solutions. Otherwise, these peptides were not water soluble. These concentrated solutions were diluted to desired concentration by adding Milli-Q water, or phosphate buffered saline buffer (100×10^{-3} M KH₂PO₄, 10×10^{-3} M Na₂HPO₄, 137×10^{-3} M NaCl, 2.7×10^{-3} M KCl, pH 7.4). These peptides were filtered through a 0.22 μ m filter to remove the insoluble particles.

Dynamic Light Scattering

DLS experiments were performed on a PDDLS/Batch DLS instrument (Precision Detectors, Franklin, MA) with 200 μ L of the peptide solution for a log 2 series of concentrations. The scattered

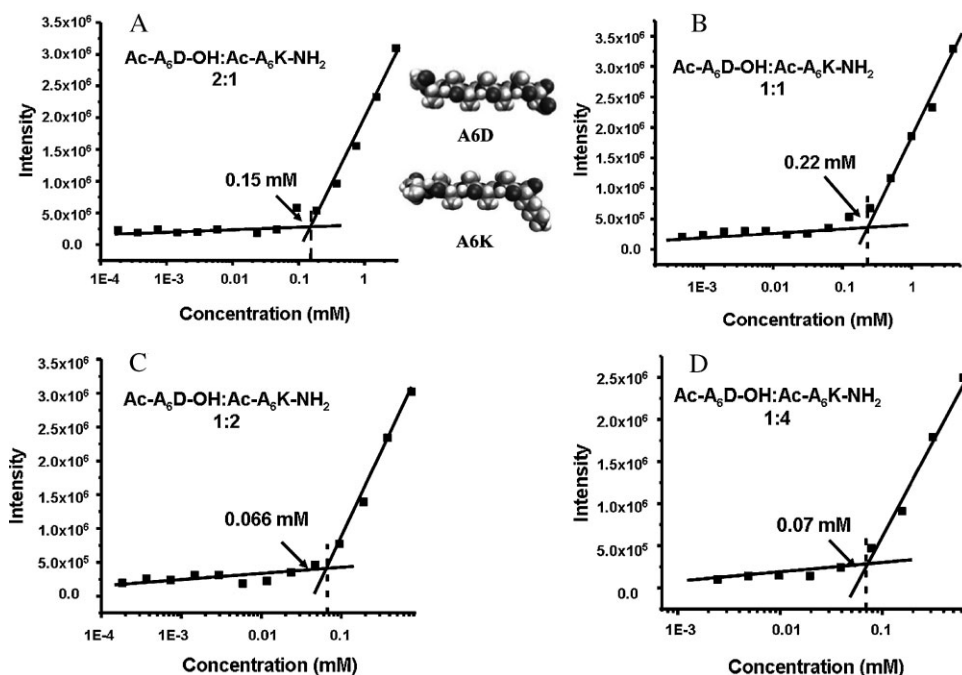


Figure 1. The intensity of the light scattering from the solution containing Ac-A₆D-OH and Ac-A₆K-NH₂ as function of concentration of total peptides in 1×10^{-3} M. The CAC in water was observed through the intersection of the two lines in different concentration regions. (A) The CAC value is 0.15×10^{-3} M for the molar ratio of Ac-A₆D-OH/Ac-A₆K-NH₂ = 2:1. The inset shows the molecular models for the Ac-A₆D-OH and Ac-A₆K-NH₂. (B) The CAC value is 0.24×10^{-3} M for the molar ratio of Ac-A₆D-OH/Ac-A₆K-NH₂ = 1:1. (C) The CAC value is 0.066×10^{-3} M for the molar ratio of Ac-A₆D-OH/Ac-A₆K-NH₂ = 1:2. (D) The CAC value is 0.07×10^{-3} M for the molar ratio of Ac-A₆D-OH/Ac-A₆K-NH₂ = 1:4.

light was collected at a 90° angle and the intensity of the scattered light was acquired by a Precision Deconvolve program.

Atomic Force Microscopy

For AFM experiments, 3 μ L of sample solution for various concentrations was deposited onto a freshly cleaved mica surface and then air-dried before AFM imaging. The images were obtained at ambient temperature conditions using AFM (Nanoscope IIIa and Dimension 3100, Veeco Metrology, USA) operated in tapping mode. The cantilevers used in AFM imaging are silicon cantilevers with typical spring constant of $30 \text{ N} \cdot \text{m}^{-1}$ and resonant frequency of 280 kHz. Images are flattened for better illustration.

Results and Discussion

The Critical Aggregation Concentration for the Mixed Peptide Surfactants

Dynamic light scattering is a technique used for particle sizing of samples, typically in the sub-micron range. The CACs of a wide range of surfactants have been routinely measured by DLS method because the light scattering intensities are correlated with the surfactant aggregation

sizes. When the concentration is lower than their CACs, the surfactants are mostly monomer and/or in small clusters, so the light scattering intensity is negligible. When micelles or other kind of self-assembly structures start to form above their CACs, the light scattering intensities undergo dramatic increase as function of surfactant concentration increases. By using this method, the CACs of Ac-A₆D-OH and Ac-A₆K-NH₂ have been obtained in water and buffer solutions. For example, in water, Ac-A₆D-OH has a CAC of $\approx 0.46 \times 10^{-3}$ M, and Ac-A₆K-NH₂ has a CAC of $\approx 0.93 \times 10^{-3}$ M, which are consistent with the CAC values reported previously (Ac-A₆D-OH: $\approx 0.46 \times 10^{-3}$ M and Ac-A₆K-NH₂: $\approx 1.02 \times 10^{-3}$ M^[9]). However, in PBS buffer solution, Ac-A₆D-OH

has a CAC of $\approx 0.22 \times 10^{-3}$ M, and Ac-A₆K-NH₂ has a CAC of $\approx 0.15 \times 10^{-3}$ M, which also agree well with the CACs reported by Nagai et al.^[9] for Ac-A₆D-OH $\approx 0.30 \times 10^{-3}$ M and Ac-A₆K-NH₂ $\approx 0.14 \times 10^{-3}$ M.

The same behavior is shown in Figure 1 for the mixed peptides. For all the mixed peptide solutions, the concentrations of the solutions are assigned to be the total peptide concentrations. From the intersection of the two lines, the CAC value was obtained to be 0.15×10^{-3} M for the molar ratio of Ac-A₆D-OH/Ac-A₆K-NH₂ = 2:1 (Figure 1A), $\approx 0.22 \times 10^{-3}$ M for the molar ratio of Ac-A₆D-OH/Ac-A₆K-NH₂ = 1:1 (Figure 1B), and $\approx 0.066 \times 10^{-3}$ M for the molar ratio of Ac-A₆D-OH/Ac-A₆K-NH₂ = 1:2 (Figure 1C), and, and 0.07×10^{-3} M for Ac-A₆D-OH/Ac-A₆K-NH₂ = 1:4 (Figure 1D). The CAC values of the mixed peptide solutions for all the four molar ratios decrease significantly than those of the solutions consisting individual Ac-A₆D-OH or Ac-A₆K-NH₂ peptides. The minimum CAC was obtained at the molar ratio of Ac-A₆D-OH/Ac-A₆K-NH₂ = 1:2, in which the total amount of the positive charges and negative charges is nearly the same in the solution. The dramatic decrease in the CAC can be attributed to the synergistic effect of the mixture of cationic and anionic surfactants due to the reduced electrostatic repulsion between them.^[15,16]

Table 1. The CAC values for mixed peptides with different molar ratios in water and PBS buffer solution.

Ac-A ₆ D-OH/ Ac-A ₆ K-NH ₂ (molar ratio)	1:0	2:1	1:1	1:2	1:4	0:1
CACs in Water ($\times 10^{-3}$ M)	0.46	0.15	0.22	0.066	0.07	0.93
CACs in PBS ($\times 10^{-3}$ M)	0.22	0.18	0.36	0.105	0.205	0.15

The CAC values for the mixed peptide solution are also measured using DLS in the PBS solution (Table 1). The CAC value is $\approx 0.18 \times 10^{-3}$ M for the molar ratio of Ac-A₆D-OH/Ac-A₆K-NH₂ = 2:1, $\approx 0.36 \times 10^{-3}$ M for the molar ratio of Ac-A₆D-OH/Ac-A₆K-NH₂ = 1:1, $\approx 0.105 \times 10^{-3}$ M for the molar ratio of Ac-A₆D-OH/Ac-A₆K-NH₂ = 1:2, and 0.205×10^{-3} M for the molar ratio of Ac-A₆D-OH/Ac-A₆K-NH₂ = 1:4. The minimum CAC for the mixed peptide solution was also obtained at the molar ratio of Ac-A₆D-OH/Ac-A₆K-NH₂ = 1:2. All of the CAC values in PBS solution at different molar ratios are a little higher than those in water, which is different from the variations of the individual peptides in water and buffer solution. This difference could be explained as follows. The electrostatic repulsion between the neighboring peptides is much reduced because of the oppositely charged peptides. According to the classic packing model of the micelles for the common surfactants, there exists the electrostatic attraction between the hydrophilic heads of the neighboring peptides with opposite charges. Thus, charge screening

effect from the PBS buffer would induce the aggregation at a slightly higher concentration in accordance with the Derjaguin–Landau–Verwey–Overbeek (DLVO) theory.^[17]

It can be seen in Table 1 that the lowest CAC values are obtained for Ac-A₆D-OH/Ac-A₆K-NH₂ = 1:2 in both water and PBS solutions. These decreased CAC values reflect the free energy favored synergistic effect^[16] when the two negative charges in one Ac-A₆D-OH molecule can be totally neutralized by two positive charges of two Ac-A₆K-NH₂ molecules. This increased surface activity is helpful in stabilizing membrane proteins.^[11–13]

Nanorope Formation for Ac-A₆D-OH Assemblies

In order to study the assembly structures in the individual peptide and the mixed peptide solutions, AFM images of peptide assemblies were examined on freshly cleaved mica surface. According to the CAC values obtained from the DLS results, the peptide concentrations ranging from 1×10^{-6} M to 1×10^{-3} M of Ac-A₆D-OH solutions were used to acquire images of the assemblies. At low concentration (10×10^{-6} M), very short (100–200 nm) nanorod structures of Ac-A₆D-OH were observed aligning in one preferable direction on the mica surface (Figure 2A). This alignment can be attributed to the substrate alignment effect of mica surface. Thin layers can also be observed on the surface with a thickness of ≈ 0.2 – ≈ 0.4 nm, which suggests Ac-A₆D-OH peptide lying in self-assembled thin layers. When concentration of Ac-A₆D-OH increased to 70×10^{-6} M, short nanorods and long nanoropes with left-handedness were observed simultaneously (Figure 2B). The height of the nanorods is ≈ 0.9 nm, while the height of the nanoropes is ≈ 4 –8 nm. The helical pitch of the left-handed nanoropes is ≈ 110 nm. The helical nanorope structures for Ac-A₆D-OH

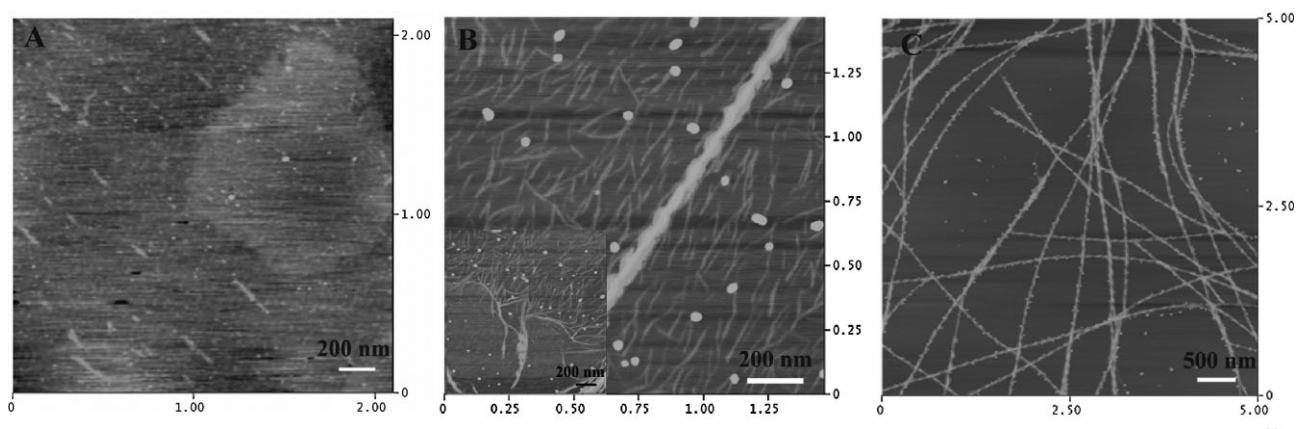


Figure 2. AFM images for the nanorod and nanorope structures of Ac-A₆D-OH on freshly cleaved mica surface at different concentrations under ambient temperature condition. (A) The concentration of Ac-A₆D-OH aqueous solution is 1×10^{-6} M. Scanning size: $2.1 \mu\text{m} \times 2.1 \mu\text{m}$, Z scale: 5 nm. (B) The concentration of Ac-A₆D-OH aqueous solution is 70×10^{-6} M. Scanning size: $1.47 \mu\text{m} \times 1.47 \mu\text{m}$, Z scale: 20 nm. The inset image illustrates the intermediate state for the twisting of nanofibrils to form the helical nanoropes. Scanning size: $1.47 \mu\text{m} \times 1.47 \mu\text{m}$, Z scale: 20 nm. (C) The concentration of Ac-A₆D-OH aqueous solution is 1×10^{-3} M. Scanning size: $5.0 \mu\text{m} \times 5.0 \mu\text{m}$, Z scale: 30 nm.

assembly have been reported by Nagai et al.,^[9] however the high-resolution images in this study detect that the nanoropes are self-assembled from many individual nanorods with smaller diameters. The inset image in Figure 2B clearly illustrates the formation mechanism of the nanoropes by twisting together of numerous nanorods. The images of the intermediate state capturing the nanorope formation process support a nucleation-growth pathway with a high degree of cooperativity similar to π -conjugated molecules.^[18,19] This new result provides a compelling mechanism to the previous reported nanotube formation for Ac-A₆D-OH^[5] using quick-freeze/deep-etch TEM images. Because of the carbon coating layer is 15–20 nm thick, so some fine features cannot be resolved in the TEM images. The helical nanoropes could be a hollow tubular structure with the tube wall consisting of twisted thin nanofibers.^[20,21]

At higher concentration (1×10^{-3} M), the nanorods disappeared; coexistence of spherical particles and tens of micron-long twisted nanoropes were observed on mica surface (Figure 2C). Because the nanoropes are very long and flexible, they would be entangled together in the solution too. So the DLS can only give the results of the apparent hydrodynamic radius, around 60–80 nm, which is larger than the diameter of the nanoropes, and much smaller than the length of the nanoropes. This suggests that the nanoropes could be a metastable structure with torsional tension along the radial axis, which serves as a driving force to twist together for the formation of the helical nanoropes. It is perhaps plausible that the tension comes from the handedness of the nanoropes even though there are no higher-resolution images of the nanorods showing handedness. Another interesting phenomenon is that the particles tend to attach on nanorope surface. Because Ac-A₆D-OH has two negative charges, the electrostatic repulsion between

Ac-A₆D-OH and negatively charged mica surface makes it difficult for the particles to be immobilized on the mica surface. The attaching of particles to the nanoropes may be an indication of the counter ions surrounding the nanorope to facilitate the stabilization of the particles.

Nanorod Formation in Ac-A₆K-NH₂ Assemblies

As a peptide surfactant with one positive charge, the assembling structures of Ac-A₆K-NH₂ in aqueous solution are different from Ac-A₆D-OH assemblies (Figure 3). At lower concentration (1×10^{-6} M), randomly distributed particles with different sizes can be observed on the surface (Figure 3A). These particles could be spherical micelles, vesicles, or aggregation of micelles on the surface. As the concentration was increased to 70×10^{-6} M, the nanorods with variable length were obtained as shown in Figure 3B. The orientation of the nanorods also shows the substrate registration feature with orientation angles of 60° or 120°. In contrast to Ac-A₆D-OH assemblies, no long nanoropes can be observed at different locations. The diameter of the nanorods is ≈ 45 nm, and the height is ≈ 3.5 nm. The identical height and variable length indicated a nanorod structure or tubular structure. Considering the tip broadening effect, the diameter of the nanorods is ≈ 17 –25 nm (assuming the curvature radius of the AFM tip is 10–15 nm), which is still much larger than the height. The difference of the smaller height and the larger diameter can be ascribed to the deformation of the nanorod or the tubular structure on the surface because of the gravity effect and also the electrostatic attraction between positive charges on outer lysine and the negatively charged mica surface. Considering the difficulties in the deformation of the nanorod with solid filling, these nanorod structures could be hollow inside. At concentrations higher than 1×10^{-3} M (Figure 3C), more

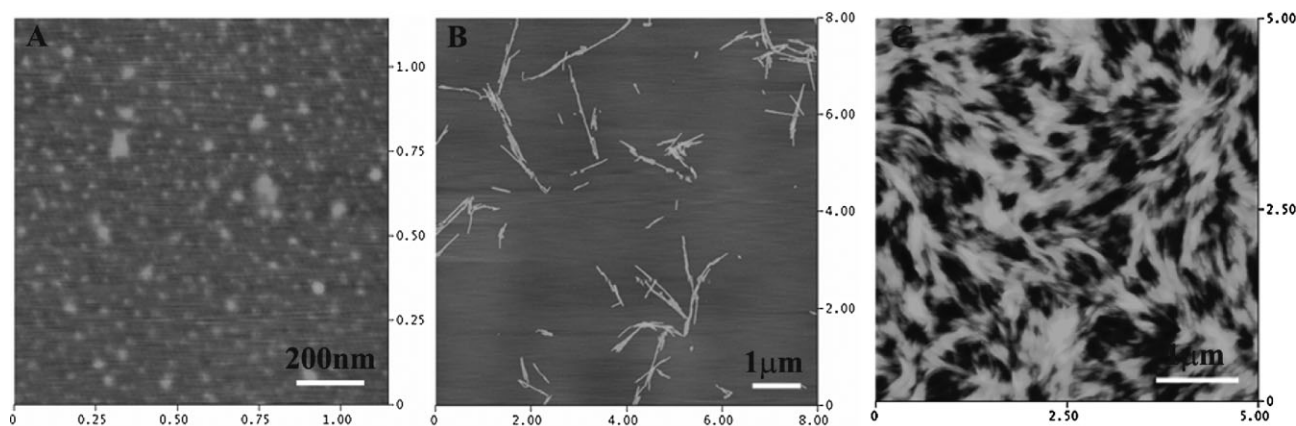


Figure 3. AFM images for the nanorod structures of Ac-A₆K-NH₂ on freshly cleaved mica surface at different concentrations under ambient conditions. (A) The concentration of Ac-A₆K-NH₂ aqueous solution is 1×10^{-6} M. Scanning size: $1.1 \mu\text{m} \times 1.1 \mu\text{m}$, Z scale: 5 nm. (B) The concentration of Ac-A₆K-NH₂ aqueous solution is 70×10^{-6} M. Scanning size: $8.0 \mu\text{m} \times 8.0 \mu\text{m}$, Z scale: 10 nm. (C) The concentration of Ac-A₆K-NH₂ aqueous solution is 1×10^{-3} M. Scanning size: $5.0 \mu\text{m} \times 5.0 \mu\text{m}$, Z scale: 20 nm.

short nanorods are stacked together forming network structure. The straight nanorod structure without twisting and entangling indicated the less tension along the radial axis, which could be attributed to the tension release by the configuration tuning of the longer flexible side chains on lysine.

Hierarchical Nanostructures in Mixed Ac-A₆D-OH and Ac-A₆K-NH₂ Peptides

Based on the synergistic effect of the mixed peptides of Ac-A₆D-OH and Ac-A₆K-NH₂ determined by DLS methods, the better assembling effect can be expected. AFM images at different concentrations ranging from 1.5×10^{-6} M to 1.5×10^{-3} M and different molar ratios (Ac-A₆D-OH and Ac-A₆K-NH₂ = 2:1, 1:1, 1:2, and 1:4) were obtained for

understanding the assembling structures and the related self-assembling mechanisms.

At lower concentration (1.5×10^{-6} M), only spherical particles can be observed for all the three molar ratios (Figure 4A–D), and the diameter of the particles is ≈ 28 nm, and the height is 1 ± 0.5 nm. The structures might be a kind of self-assembled monolayers with hydrophilic heads adsorbed on the mica surface and the hydrophobic tails aligned perpendicular to the surface with a certain tilting angle.

For the molar ratio of Ac-A₆D-OH/Ac-A₆K-NH₂ = 2:1, the assembly structures are investigated at concentration of 1.5×10^{-6} M, 15×10^{-6} M, and 1.5×10^{-3} M, respectively. Bundles of short nanorods are formed on the surface besides the spherical particles at concentration of Ac-A₆D-OH = 15×10^{-6} M. (Figure 4A). As the concentration was

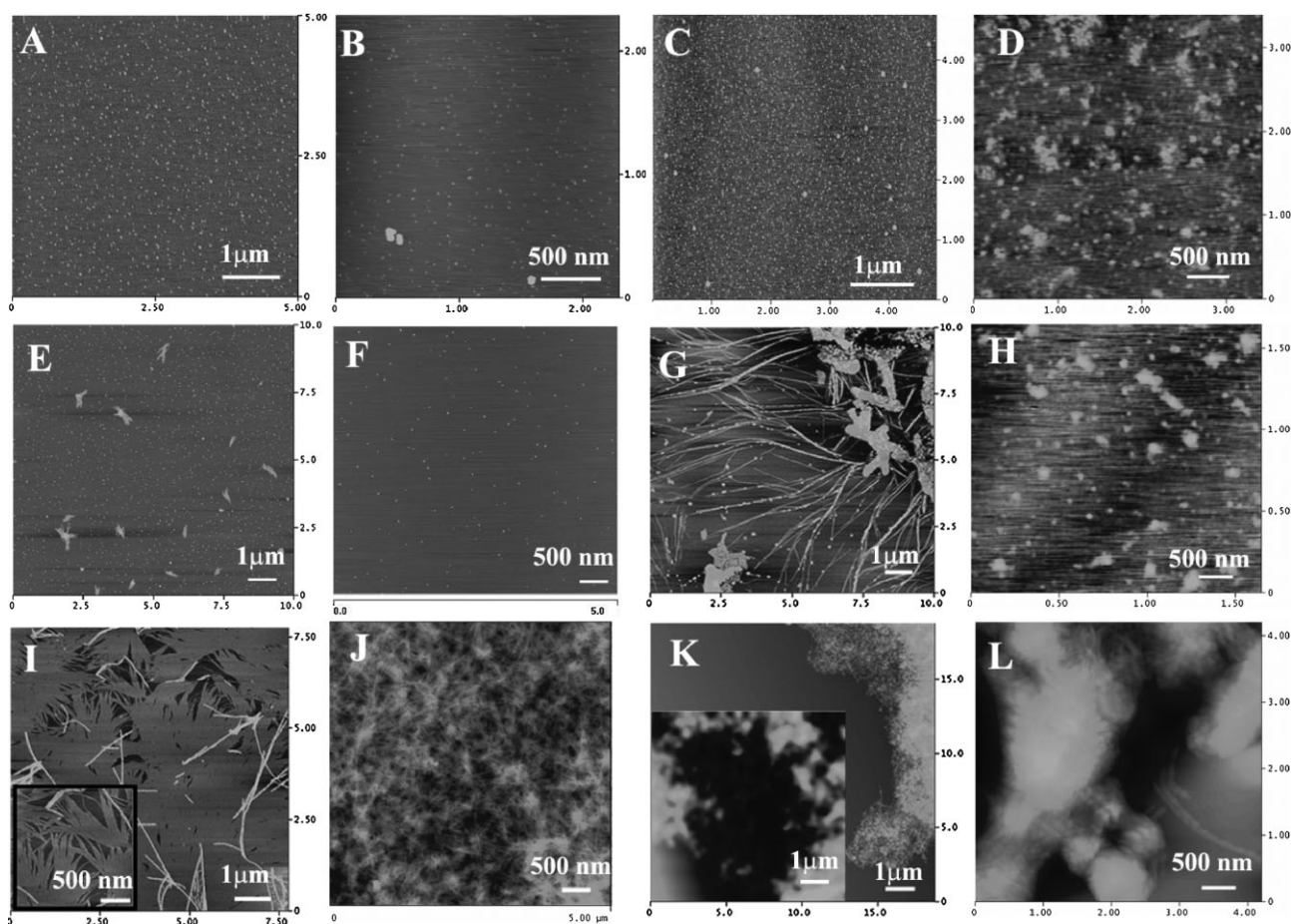


Figure 4. AFM images for the self-assembled nanostructures of mixed peptide solution containing Ac-A₆D-OH and Ac-A₆K-NH₂ on freshly cleaved mica surface at different concentrations at ambient temperature. The concentrations of the total peptides were assigned to stand for the concentration of the mixture solutions. The concentrations of the solutions are as follows, 1.5×10^{-6} M for (A), (B), (C), and (D); 15×10^{-6} M for (E), (F), (G), and (H); 1.5×10^{-3} M for (I), (J), (K), and (L). The molar ratios for the solutions are as follows, Ac-A₆D-OH/Ac-A₆K-NH₂ = 2:1 for (A), (E), and (I), and the inset in (I) is the high-resolution image showing the nanorope structure at domain boundaries; Ac-A₆D-OH/Ac-A₆K-NH₂ = 1:1 for (B), (F), and (J); Ac-A₆D-OH/Ac-A₆K-NH₂ = 1:2 for (C), (G), and (K), and the inset in (K) is the zoom-in image of the big aggregate; Ac-A₆D-OH/Ac-A₆K-NH₂ = 1:4 for (D), (H), and (L). The two white arrows point out the helical nanoropes because of the phase separation.

increased to 1.5×10^{-3} M (Figure 4I), which is well above the CAC, nanorope thin film was observed that consisted of well-aligned nanoropes with identical diameters. These nanorope thin film extended for $>90 \mu\text{m}$, which is the maximum scanning area for the AFM scanner. The small holes as defects in the packing of the nanoropes or the domain boundaries of different alignment orientation of nanoropes provided the identification of the nanorope structures in the thin film as shown in the inset zoom-in image, showing the nanorope structure at domain boundaries. Some nanoropes and nanorods on the nanorope thin film could be considered as a phase separation phenomenon, showing the helical nanoropes formed by pure Ac-A₆D-OH or the short nanorods by pure Ac-A₆K-NH₂ assemblies. The two black arrows point out the helical nanoropes because of the phase separation. From the bundles of short nanorods at concentration of 15×10^{-6} M and the thin film consisting of well-aligned nanoropes at concentration of 1.5×10^{-3} M, the high tendency of the alignment of the nanoropes was observed even for the shorter nanorods at the initial stage of nanorope formation.

For the molar ratio of Ac-A₆D-OH/Ac-A₆K-NH₂ = 1:1, only spherical particles and no obvious difference were observed for the 15×10^{-6} M concentrations (Figure 4B and F). At higher concentration (1.5×10^{-3} M), the AFM image revealed large amount of nanoropes with a diameter of ≈ 18 nm (Figure 4J), which is different from the helical nanoropes for individual Ac-A₆D-OH peptide and the short nanorod structures for individual Ac-A₆K-NH₂ peptide. The diameter of the uniform nanoropes indicated the densely packed nanostructure because of the reduced electrostatic repulsion between hydrophilic heads. The uniform nanorope formation at Ac-A₆D-OH/Ac-A₆K-NH₂ = 1:1 may be a promising scaffold system for a number of applications. For the molar ratio of Ac-A₆D-OH/Ac-A₆K-NH₂ = 1:2, where the highest synergistic effect was found from DLS results due to the lowest free energy obtained and negative charge equal to positive charges. At a concentration of 1.5×10^{-6} M (Figure 4C), more spherical particles were revealed than those with the same amount of total peptides at the other molar ratios, 2:1, 1:1, and 1:4 in Figure 4A, B, and D. The more particles formation at the same concentration of total amount of peptides showed the aggregation tendency at lower concentration, which is consistent with the synergistic effect revealed by DLS method. Some bigger particles also appeared in the image showing the tendency of earlier aggregation. At concentration of 15×10^{-6} M (Figure 4G), nanoparticles, nanoropes, and nanoplates were observed simultaneously. This early aggregation with lower uniformity demonstrated the higher aggregation speed, which can be confirmed from large aggregate formation at concentration well above the CAC (1.5×10^{-3} M in Figure 4K). The larger aggregates might be the conglomeration of nanoropes and

nanoparticles. The nanorope or nanorod-like structures could be observed in the edge of the aggregates, while they are not clearly resolved in the AFM image because of the huge height of the aggregates. The neutralization of the charges of the lysine and aspartic acid showed to the fast aggregation rate with a loss of the well organization.

For the molar ratio of Ac-A₆D-OH/Ac-A₆K-NH₂ = 1:4, bigger particles with less diameter homogeneity can be observed than those for molar ratios of 2:1, 1:1, and 1:2 (Figure 4D and H). At concentration well above the CAC, 1.5×10^{-3} M, the larger aggregates comprised of nanoropes and big particles similar to molar ratio of 1:2 indicate that the less organized aggregation with more Ac-A₆K-NH₂, which might be due to the packing difficulties for the longer flexible side chains on lysines.

From the above results at different molar ratios and different concentrations, the best synergistic effects in surface activity were achieved at the molar ratio of Ac-A₆D-OH/Ac-A₆K-NH₂ = 1:2, while the nanostructures were less organized because of the higher nucleation speed. For the molar ratio of Ac-A₆D-OH/Ac-A₆K-NH₂ = 2:1 and 1:1, uniform nanoropes with identical diameters were obtained. Interestingly, no handedness was identified from the mixed peptide systems. This phenomenon may be attributed to the tension release along the radial axis due to the configuration tuning of the flexible side chains on lysine. For the molar ratio of 1:4, the aggregation tendency is reduced compared to the neutralization state 1:2 because of more positive charges in the system, which can be proved by no nanorope formation at 15×10^{-6} M. The less organization compared to 2:1 and 1:1 indicates the more loosely packing of Ac-A₆K-NH₂ than Ac-A₆D-OH due to the flexible side chains of lysines. The well aligned nanoropes at the molar ratio of Ac-A₆D-OH/Ac-A₆K-NH₂ = 2:1 suggested the competition factor between the electrostatic repulsion according to DLVO theory^[17] and the hydrophobic interaction arising from the long side chains on lysine residues. The less the total charges there are, the faster the aggregation speed is, but the less organized the nanostructures become. So well-aligned nanoropes can be obtained by exquisitely fine-tuning the charges and the hydrophobic interaction in the peptide mix, which provide a new avenue for designing new nanomaterials.

Assembling Mechanism of the Mixed Peptides

Based on the above discussion of DLS and AFM results, we propose a plausible assembling mechanism to explain the observed aggregation process of the nanorope structure in the mixed peptide population. At lower concentration well below the CAC value, Ac-A₆D-OH and Ac-A₆K-NH₂ are randomly oriented and distributed as monomers in solution (Figure 5A). The cyan sticks represent the hydrophobic tails

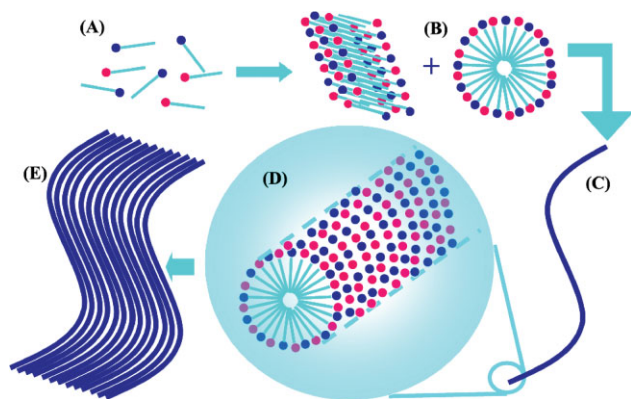


Figure 5. A proposed plausible mechanism for the assembly process of the nanorope structure. (A) The randomly oriented and distributed peptide monomers at low concentration, the color code: cyan sticks represent the hydrophobic tails consisting of six alanine residues; red balls represent the hydrophilic head aspartic acid of Ac-A₆D-OH with two negative charges; the blue balls represent the hydrophilic head lysine Ac-A₆K-NH₂ with one positive charge. (B) The spherical particle formation or nanorod structure. (C) The formation of the nanorope structure. (D) The schematic illustration of the section structure of the nanoropes. (E) The alignment of the numerous nanoropes leading to the formation the thin film.

consisting of six alanine residues; the red balls denote the hydrophilic head aspartic acid of Ac-A₆D-OH with two negative charges; the blue balls for the hydrophilic head of lysine Ac-A₆K-NH₂ with one positive charge. Because of the electrostatic attraction between opposite charges and the hydrophobic interactions between alanine tails, the interdigitated short and thin nanorods, or spherical particles, could be formed in the solution (Figure 5B). The negatively charged and positively charged peptides tend to position themselves alternatively for lowering the energy associated with the electrostatic interaction. At higher concentration, the nanoropes can be formed which can be considered as an extended structure of the spherical particles (Figure 5C and D). When the molar ratios of the two peptides are at an appropriate concentration, the fine-tuning of the charges and the hydrophobic interaction would produce the alignment of the nanoropes into thin film.

Conclusion

The self-assembly structures and the associated mechanism were studied using DLS and AFM techniques. The best synergistic effect was obtained at the molar ratio of Ac-A₆D-OH/Ac-A₆K-NH₂ = 1:2 by DLS measurements. Uniformed nanoropes were observed in AFM images at the molar ratio of Ac-A₆D-OH/Ac-A₆K-NH₂ = 1:1, and the nanothin film formation with aligned nanoropes was

reported at a molar ratio of 2:1. The well aligned nanoropes at a molar ratio of Ac-A₆D-OH/Ac-A₆K-NH₂ = 2:1 indicated the competition factor between the electrostatic repulsion according to the DLVO theory^[17] and the hydrophobic interaction arising from the long side chains on lysine residues. This study will be valuable for designing new nanomaterials based on mixing different ratios of designer lipid-like peptide surfactants.

Acknowledgements: This work is supported in part by the *National Science Foundation* grant CCR-0122419 to the MIT Center for Bits and Atoms of the Massachusetts Institute of Technology. Mr. U. G. K. Khoe gratefully thanks *Kartini Muljadi* for generous financial support. Dr. Y. L. Yang is partially supported by the *National Basic Research Program of China* (973 Program, grant no. 2006CB936802) and *K. C. Wong Education Foundation*, Hong Kong.

Received: June 30, 2008; Revised: August 3, 2008; Accepted: August 5, 2008; DOI: 10.1002/mabi.200800182

Keywords: atomic force microscopy (AFM); dynamic light scattering; peptides; self-assembly; surfactants

- [1] S. Zhang, *Nat. Biotechnol.* **2003**, *21*, 1171.
- [2] E. Gazit, *Chem. Soc. Rev.* **2007**, *36*, 1263.
- [3] E. H. Koo, P. Lansbury, J. Kelly, *Proc. Natl. Acad. Sci. USA* **1999**, *96*, 9989.
- [4] M. Goedert, M. G. Spillantini, *Science* **2006**, *314*, 777.
- [5] S. Vauthey, S. Santoso, H. Gong, N. Watson, S. Zhang, *Proc. Natl. Acad. Sci. USA* **2002**, *99*, 5355.
- [6] S. Santoso, W. Hwang, H. Hartman, S. Zhang, *Nano Lett.* **2002**, *2*, 687.
- [7] G. von Maltzahn, S. Vauthey, S. Santoso, S. Zhang, *Langmuir* **2003**, *19*, 4332.
- [8] S. Yang, S. Zhang, *Supramol. Chem.* **2006**, *18*, 389.
- [9] A. Nagai, Y. Nagai, H. Qu, S. Zhang, *J. Nanosci. Nanotechnol.* **2007**, *7*, 1.
- [10] P. Kiley, X. Zhao, M. Vaughn, M. A. Baldo, B. D. Bruce, S. Zhang, *PLoS Biol.* **2005**, *3*, 1180.
- [11] J. Yeh, S. Du, A. Tordajada, J. Paulo, S. Zhang, *Biochemistry* **2005**, *44*, 16912.
- [12] X. Zhao, Y. Nagai, P. Revees, P. Kiley, H. G. Khorana, S. Zhang, *Proc. Natl. Acad. Sci. USA* **2006**, *103*, 17707.
- [13] K. Matsumoto, S. Koutsopoulos, M. Vaughn, B. D. Bruce, S. Zhang, *J. Phys. Chem.* **2008** (in press).
- [14] A. Yagmur, P. Laggner, S. Zhang, M. Rappolt, *PLoS One* **2007**, *2*, e479.
- [15] J. N. Israelachvil, D. J. Mitchell, B. W. Ninham, *J. Chem. Soc. Faraday Trans. II* **1976**, *72*, 1525.
- [16] M. Bergström, J. C. Eriksson, *Progr. Colloid Polym. Sci.* **2004**, *123*, 16.
- [17] E. J. W. Verwey, J. T. G. Overbeek, *Theory of the Stability of Lyophobic Colloids*, Elsevier, Amsterdam 1948, pp. 106–115.
- [18] O. Carny, D. Shalev, E. Gazit, *Nano Lett.* **2006**, *6*, 1594.
- [19] M. Reches, E. Gazit, *Nat. Nanotech.* **2006**, *1*, 195.
- [20] P. Jonkheijm, P. van der Schoot, A. P. H. J. Schenning, E. W. Meijer, *Science* **2006**, *313*, 80.
- [21] M. Wang, Y.-L. Yang, C. Wang, *J. Phys. Chem. C* **2007**, *111*, 6194.